inter.noise
HAMBURG 2016

Impact sound insulation: Transient power input from the rubber ball on locally reacting mass-spring systems

Susumu HIRAKAWA[1]; Carl HOPKINS[2]; Pyoung Jik LEE[3]

Acoustics Research Unit, School of Architecture, University of Liverpool, UK

ABSTRACT

For heavy impacts in heavyweight buildings, impact sound insulation is measured using the rubber ball but little is understood about the interaction of the rubber ball with a floating floor. This paper describes experimental work to investigate idealised floating floors using a steel plate on different resilient materials to represent a locally-reacting mass-spring system. Force plate measurements show that there are two characteristic force-time pulses from the mass-spring systems, a single and double hump for low and high stiffness springs respectively. These trends are shown to occur with a mass-spring model for both the rubber ball and the mass-spring system when implemented in Matlab Simulink but only with optimized material properties. With excitation from the rubber ball with and without a mass-spring system, $L_{v,\mathrm{Fmax}}$ measurements on a concrete base floor and $L_{p,\mathrm{Fmax}}$ measurements in a receiving room indicate that the change in transient power measured using the force plate and the change in $L_{v,\mathrm{Fmax}}$ or $L_{p,\mathrm{Fmax}}$ are only similar when the resilient material in the mass-spring system is dynamically stiff.

Keywords: Impact sound insulation, ISO rubber ball I-INCE Classification of Subjects: 41.3 45

1. INTRODUCTION

Low-frequency impact sounds generated by footsteps can cause annoyance in high-rise heavyweight buildings (1). To assess heavy impacts such as footsteps, the measurement protocol using the standard rubber ball is described in International Standards (2,3) Japanese Standards (4) and Korean Standards (5). These require measurement of the Fast time-weighted maximum sound pressure level, $L_{p,\mathrm{Fmax}}$, in rooms; hence there is a need for a prediction model that can estimate this parameter.

Robinson and Hopkins (6, 7) have shown that Transient Statistical Energy Analysis (TSEA) can be used to predict Fast time-weighted sound pressure levels ($L_{\mathrm{p,Fmax}}$) in heavyweight buildings due to both direct and flanking transmission. More recent work (8) shows that TSEA can be used to predict $L_{\mathrm{p,Fmax}}$ in rooms due to excitation directly onto a concrete floor from the standard rubber ball and human footsteps, even in the low frequency-range. This TSEA model requires a transient power input (6) from the excitation source. For the rubber ball this power input can be calculated from the measured blocked force and the driving-point mobility of the receiver structure. However, the validation with the rubber ball has only been carried out with excitation of a concrete floor slab (8).

To extend the use of TSEA to typical building structures it is necessary to consider impacts on a floating floor that is supported by the concrete floor slab. For rubber ball impacts it might be possible to either predict the transient power input injected into the rigid walking surface of a floating floor or into the concrete base floor which supports it. The latter is likely to be advantageous because the vibrational response of a floating floor is strongly coupled to the base floor, particularly in the low frequency range near the mass-spring resonance.

Previous research into prediction of the blocked force applied by a non-standard ball and the bang machine on a concrete floor used a mass-spring damper model (9,10). A model for the bounce of a hollow elastic spherical shell on a rigid surface was proposed by Hubbard and Stronge (11). This requires solving a second-order differential equation for a hollow elastic spherical shell impacting upon a rigid surface. Schoenwald *et al* (12) applied this model to the standard rubber ball and showed that the blocked force could be predicted in the 31.5 Hz and 63Hz octave bands, but there were large

[1] S.Hirakawa@ liverpool.ac.uk
[2] Carl.Hopkins@liverpool.ac.uk
[3] P.J.Lee@liverpool.ac.uk

differences in higher frequency bands when compared with measurements; this could be due to the fact that it does not incorporate the modal response of the ball. A modal approach which could account for the ball resonances was introduced by Park *et al* (13) which could predict the blocked force for the bang machine below 50 Hz and the standard rubber ball up to 200 Hz.

As a first step before considering the introduction of floating floors into a TSEA model, this paper uses an experimental approach to gain insights into a locally reacting mass-spring system which represents an idealization of a floating floor. This approach is convenient because (a) the small dimensions of the system allow a force plate to be used to measure the force input using the rubber ball, with and without the mass-spring system and (b) the results can be compared with a Matlab Simulink model based on lump mass-spring systems. The difference between the measured transient power with and without the mass-spring system is then compared to measurements with a concrete floor above a room in terms of the difference in $L_{p,\mathrm{Fmax}}$ (in the room) and $L_{v,\mathrm{Fmax}}$ (on the concrete floor) with and without the mass-spring system on the concrete floor.

2. Constructions

2.1 Test room

Measurements have been carried out using a small test room with a 125 mm thick concrete floor above it as shown in Figure 1. The lowest room mode is 60 Hz and the lowest bending mode of the floor is 84 Hz. The use of a small room is useful as it allows an assessment of the effect of the mass-spring resonance frequency in relation to the fundamental mode of the floor, but it is expected that when making comparisons with force plate measurements of transient power with and without the mass-spring system the agreement might be affected by low mode counts.

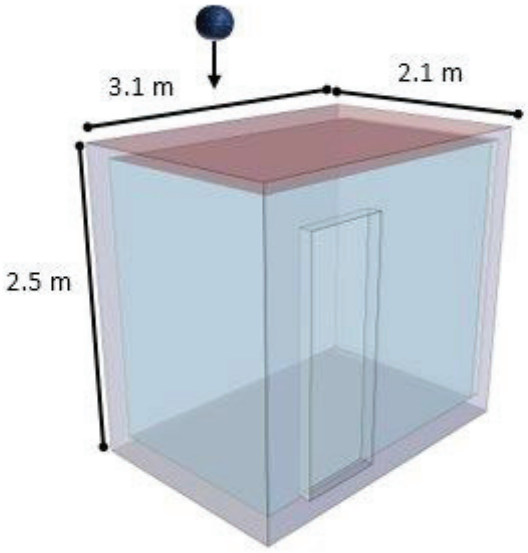

Figure 1. Small test room

2.2 Mass-spring systems

Seven locally reacting mass-spring systems are formed from a 20 mm thick steel plate (200 mm x 200 mm) on seven different resilient materials. The dynamic stiffness of these resilient materials is determined following the general approach described in ISO 29052 (14) but using a force hammer to apply a peak force of 1500N±50N that is similar to that applied by the rubber ball. The internal loss factor of the resilient material is determined from the 3dB down points of the magnitude of the driving-point mobility measured to determine the dynamic stiffness. The properties of the resilient materials are given in Table 1. All of the resilient materials can be assumed to have a reasonably uniform stiffness over the 200 mm x 200 mm area except material A which was made from recycled foam.

Table 1. Properties of the resilient material samples.

Sample (Resilient Material)	Sample thickness (mm)	Dynamic stiffness per unit area (MN/m^3)	Internal Loss Factor (-)	Mass spring resonance frequency (Hz)
A (Recycled Foam)	15	5.5	0.27	30
B (EPS* - M20)	28	10.3	0.21	41
C (EPS* - M40)	28	18.5	0.33	55
D (Yellow Sylomer)	15	25.1	0.47	64
E (Green Sylomer)	15	32.6	0.32	73
F (EVA* - 5)	20	41.2	0.61	82
G (EVA* - 4)	20	89.6	0.55	121

* EPS is expanded polystyrene and EVA is ethylene-vinyl acetate.

3. Methods

3.1 Calculation of the transient power input

TSEA requires a transient power input for the impact source such as the standard rubber ball (8). For a rubber ball (source) impacting a concrete base floor (receiver), the source mobility is higher than the receiver mobility (i.e. $|Y_S| >> |Y_R|$) and a time-varying power input can be determined as a hybrid transient power input from the measured blocked force using (6)

$$W_{\mathrm{in},i} = F_{\mathrm{rms}}^2 \mathrm{Re}\{Y_{\mathrm{dp}}\} \qquad (1)$$

where F_{rms} is the rms force determined using measurements with a force plate and Y_{dp} is the driving-point mobility of the floor slab (measured or predicted).

For a rubber ball impact onto a floating floor (or mass-spring system) on a concrete base floor, the source mobility that is 'seen' by the concrete floor is the combination of the rubber ball and the floating floor (or mass-spring system). For some floating floors (or mass-spring systems), $|Y_S| > |Y_R|$ rather than $|Y_S| >> |Y_R|$ and it is possible that $|Y_S| \approx |Y_R|$ at certain frequencies. For this reason a range of different resilient materials are used to create different mass-spring systems for this paper.

3.2 Force plate measurements

The force plate is constructed from two 35mm thick circular steel plates (m_1=m_2=26.4 kg) with a radius of 175 mm as indicated in Figure 2. The force is measured by summing the output from three Kistler 9041A force transducers that are bolted between the two steel plates. The force-time spectrum was measured using the B&K PULSE Labshop system with a time resolution of 61.04 µs and an Energy Spectral Density (ESD) with a frequency resolution of 1 Hz. The force time spectrum was converted to one-third octave bands by summing the discrete frequency data within the upper and lower limits of the one-third octave band.

The force plate was used to measure the mean-square force with (a) a rubber ball impact using a drop height of 1 m and (b) the same rubber ball impact on top of the mass-spring system (see Figure 2).

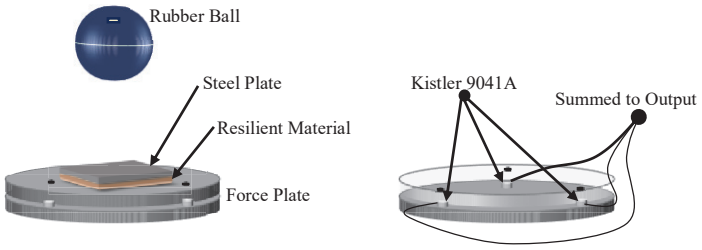

Figure 2. Force plate showing force washers (left) and supporting the mass-spring system (right).

3.3 Measurements using a small test room with concrete floor

$L_{p,\mathrm{Fmax}}$ and $L_{v,\mathrm{Fmax}}$ are measured using the concrete floor with and without the mass-spring system. The mass-spring system used the same seven different resilient materials. For each of five excitation positions, two accelerometers (B&K Type 4371) and two sound level meters (B&K Type 2231) were used at different positions. The results at each position were an average of five ball drops from a height of 1 m. All measurements were taken using the B&K PULSE Labshop system.

3.4 Prediction of forces using mass-spring models

Assuming a linear time invariant system, Matlab Simulink (15, 16) is used to model the rubber ball falling freely onto (a) the force plate and (b) a locally reacting mass-spring system on the force plate. These situations are indicated in Figure 3.

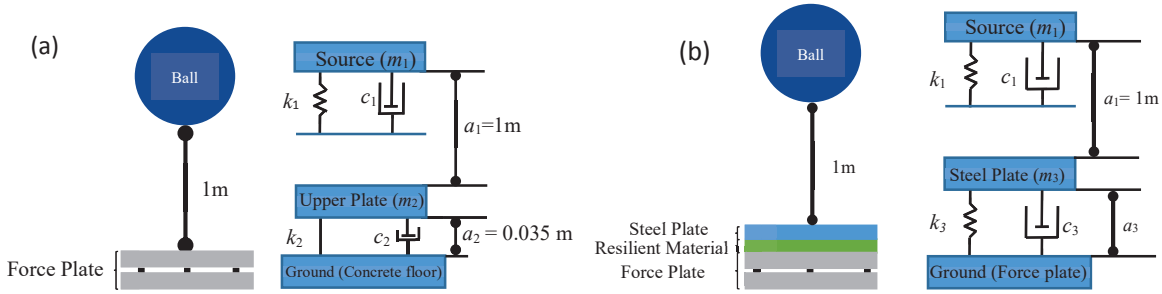

Figure 3. Mass-spring models for the rubber ball falling freely onto (a) the force plate and (b) a locally reacting mass-spring system on the force plate.

Two aspects are considered, firstly when the ball and the surface are independent, and secondly when they are coupled after impact. Before impact each mass acts independently, then when the rubber ball collides with the surface they move together and the ball deforms, then leaves the surface to become independent again. For the coupled situation, the dynamics consider the elastic properties of the ball. This is the phase when blocked force is determined. For model (a), using the initial conditions: $y_1 = a_1$, $\dot{y}_1=0$, $y_{2(3)}=a_{2(3)}$, $\dot{y}_{2(3)}=0$, the following equations of motion can be solved

$$m_1\ddot{y}_1 + c_1\left(\dot{y}_1 - \dot{y}_{2(3)}\right) + k_1\left(y_1 - y_{2(3)} - a_1\right) = -\mathrm{m}_1 g \qquad (2)$$

$$m_{2(3)}\ddot{y}_{2(3)} + c_{2(3)}\dot{y}_{2(3)} + k_{2(3)}\left(y_{2(3)} - a_{2(3)}\right) - c_1\left(\dot{y}_1 - \dot{y}_{2(3)}\right) - k_1\left(y_1 - y_{2(3)} - a_1\right) = -m_{2(3)}g \qquad (3)$$

Subscript 2 in the initial conditions, equations 2 and 3 replaced to 3 for model (b).

g is the acceleration due to gravity, m_1 is the mass of the rubber ball, m_2 is the mass of the force plate for model (a), m_3 is the mass of the steel plate for model (b), k_1 is the stiffness of the rubber ball, and k_2 is the combined stiffness of the force washers for model (a) and k_3 is the stiffness of the resilient material in the mass-spring system for model (b), a_1 is the diameter of rubber ball, a_2 is the thickness of the force washers for model (a), a_3 is the thickness of the resilient material for model (b).

The variables c_1, c_2 and c_3 describe the damping coefficient associated with the springs. For a mass-spring system this can be calculated using

$$c_i = \eta_i\sqrt{k_i m_i} \qquad (4)$$

Where η_i is the internal loss factor and subscripts also correspond with the springs.

Figure 4 shows the force equilibrium diagram where source indicates the rubber ball and receiver indicates either the force plate or mass-spring system. The blocked force acting on the receiver is calculated according to

$$\begin{aligned} F = m_{2(3)}g &= m_{2(3)}\ddot{y}_{2(3)} - c_1\left(\dot{y}_1 - \dot{y}_{2(3)}\right) - k_1\left(y_1 - y_{2(3)} - a_1\right) \\ &= c_{2(3)}\dot{y}_{2(3)} + k_{2(3)}\left(y_{2(3)} - a_{2(3)}\right) \end{aligned} \qquad (5)$$

Again, replace subscript 2 to 3 for model (b).

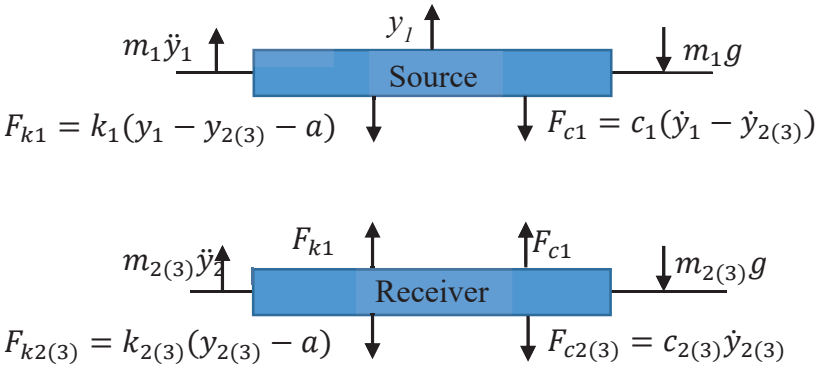

Figure 4. Force equilibrium.

3.5 Driving-point mobility of the mass-spring systems

Figure 5 shows measured driving-point mobilities of the rubber ball, mass-spring systems (with excitation on the steel plate) and the 125 mm concrete floor. This confirms that the rubber ball has a significantly higher mobility than the concrete floor; hence in this case considering a blocked force to determine the transient power is reasonable. For the mass-spring systems the peaks in the driving-point mobilities correspond to the mass-spring resonances calculated from the measured dynamic stiffness. As these mobilities tend to be at least 20 dB higher than the concrete floor it is also reasonable to consider blocked forces.

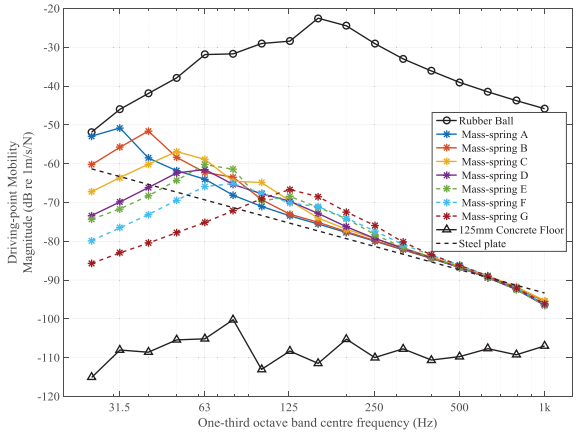

Figure 5. Driving-point mobility of the rubber ball, mass-spring systems and the concrete floor

3.6 Force plate measurements with and without the mass-spring systems

Figure 6 shows the measured force for the rubber ball impact on mass-spring system with resilient materials in terms of force versus time and the ESD. For comparison the graphs also show the results for the rubber ball impacting directly onto the force plate.

For the mass-spring systems with resilient materials A to D, the measured force has a single hump in the time domain but compared to the direct measurement the shape of the rising curve is significantly altered, the peak force is significantly increased and the time at which the peak force occurs is increased. For the mass-spring systems with resilient materials E to G the measured force has a double hump and although the peak force is higher (≈200 N) than the direct measurement the peak force is not as high as with materials A to D. The force versus time curves indicate that the resilient materials can be considered in two groups: Group 1 (A, B, C, D) with low dynamic stiffness where there is a single hump and Group 2 (E, F, G) with high dynamic stiffness with a double hump.

In the frequency domain there is no clear link between the mass-spring resonance frequencies for the different resilient materials (see Table 1) and the frequency bands in which the ESD is higher than the direct measurement. For mass-spring systems with Group 2 materials, the ESD is similar to the direct measurement up to the 63 Hz band, but significantly higher in the 125, 160 and 200 Hz bands.

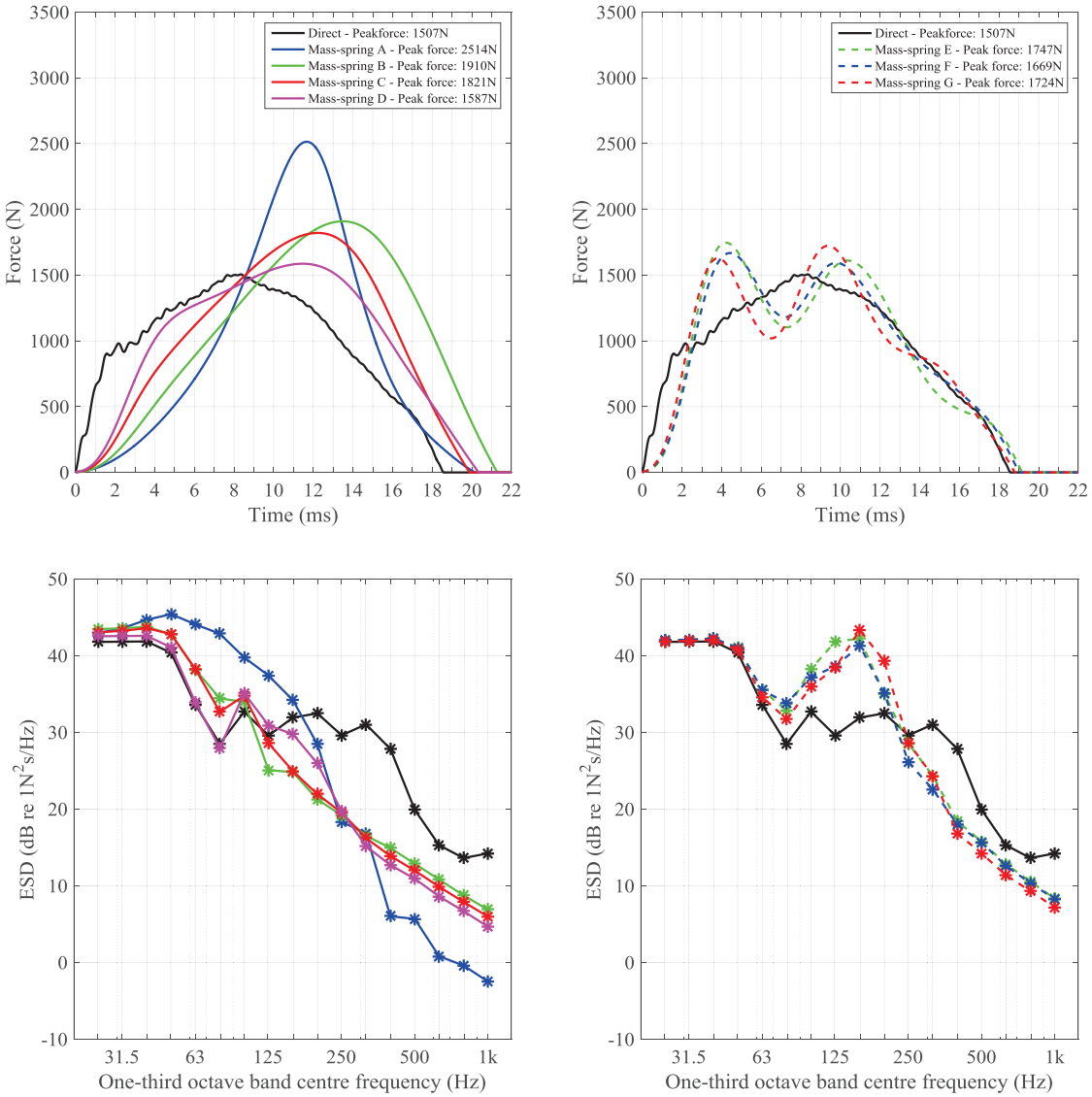

Figure 6. Measured mass-spring systems with resilient materials A, B, C and D (Left) and E, F and G (Right): Force versus time (Upper graphs) and ESD in one-third octave bands (Lower graphs).

3.7 Comparison of measured and simulated forces for the mass-spring systems

Figure 7 shows the simulated force versus time curves for comparison with the measured values that were shown in Figure 4. For the rubber ball impact on a rigid surface the blocked force from the simulation and measurement have the same general shape and duration with ripples on the rising curve. For impacts on the mass-spring systems with Group 1 materials, the simulation shows the same general features as the measurement but it does not accurately predict the response. For example, the predicted peak force for resilient material A is significantly lower than the measurement. For Group 2 materials the simulation did not reproduce the double hump seen in the measurements.

Comparison of the measured and simulated ESD shows that the differences are <10dB for Group 1 resilient materials (except resilient material A) between 25 Hz and 1000 Hz. For resilient material A, the difference is >10 dB above 300 Hz. For Group 2 resilient materials, there is only agreement within 10 dB between 25 Hz and 100 Hz, and between 300 Hz and 1000 Hz.

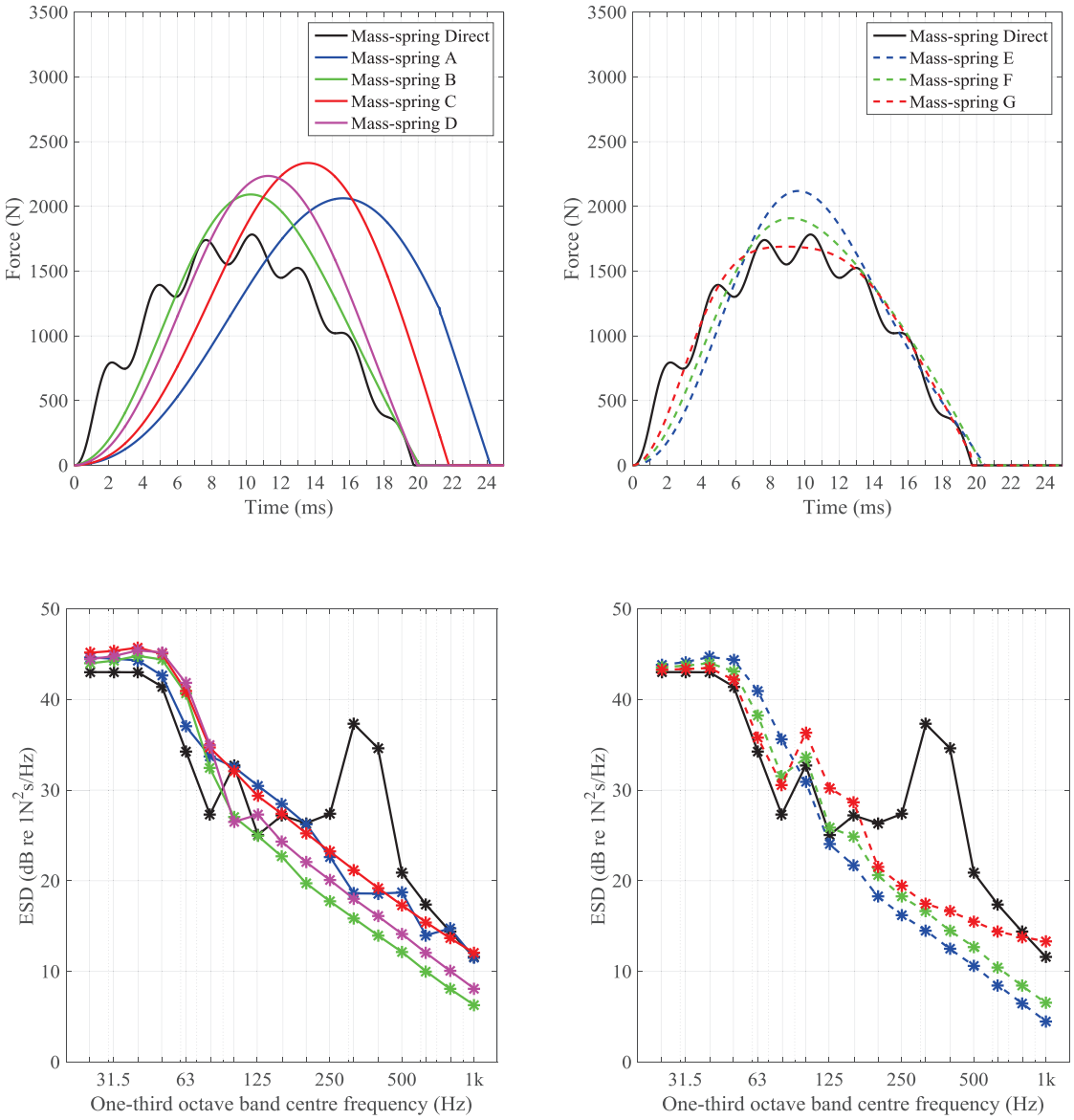

Figure 7. Simulated mass-spring systems with resilient materials A, B, C and D (Left) and E, F and G (Right): Force versus time (Upper graphs) and ESD (Lower graphs)

For Group 2 resilient materials the simulation has the potential to emulate the double hump feature in the force time curve that was observed in the measurements. However this requires altering the stiffness and damping values for each material as indicated in Table 2. Comparison of measurements with the optimized simulation is shown in Figure 8 with close agreement between the curves. However, the optimized values used to give such good agreement are significantly different to those that were measured (see Table 1). For the optimized simulation, the measured stiffness of the Group 2 resilient materials is increased by a factor of 1.8 to 3.9 times and the measured damping coefficient is increased by a factor of 1.15 to 2.6 times. The change to the stiffness of the rubber ball was negligible, but the damping coefficient was increased from 26 to 100.

Figure 9 shows the difference between measured ESD and the optimized simulation of ESD. The optimized simulation reproduces the ESD to within 5 dB between 25 Hz and 1000 Hz.

Table 2. Optimized stiffness and damping parameters used in the simulation

Sample (Resilient Material)		k_1 (N/m)	c_1	k_3 (MN/m^3)	c_3
E	Measured	6.16×10^4	26	32.6	917
	Optimized	6.16×10^4	100	130	800
F	Measured	6.16×10^4	26	41.2	1964
	Optimized	6.1×10^4	100	140	1200
G	Measured	6.16×10^4	26	89.6	2613
	Optimized	6.1×10^4	100	163	1000

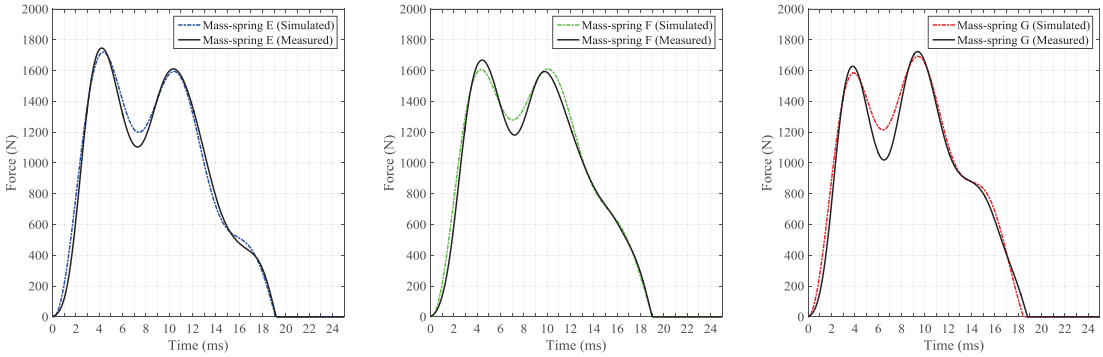

Figure 8. Measured and optimized simulation of force versus time for Group 2 resilient materials.

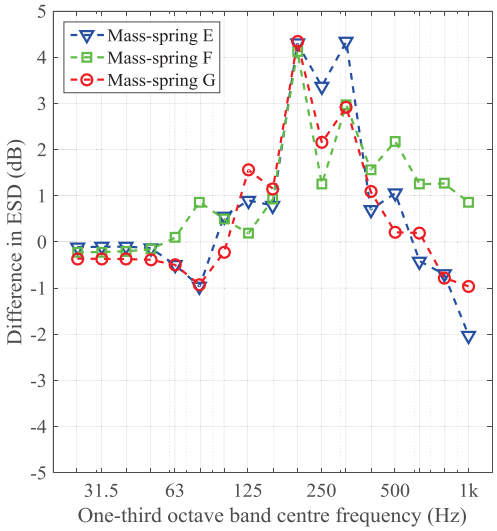

Figure 9. Difference between the optimized simulation and measured ESD for Group 2 resilient materials.

3.8 Relationship between the force plate and room measurements

To assess the relationship between the force plate measurements and the room measurements, the difference between the measured transient power with and without the mass-spring system that was measured using the force plate is compared to the difference in $L_{p,\mathrm{Fmax}}$ and $L_{v,\mathrm{Fmax}}$ with and without the mass-spring system. The difference in the measured transient power input due to the mass-spring systems is ΔW_{in} (without minus with the mass-spring system). The differences in the measured $L_{\mathrm{p,Fmax}}$ and $L_{\mathrm{v,Fmax}}$ (without minus with the mass-spring system), $\Delta L_{p,\mathrm{Fmax}}$ and $\Delta L_{v,\mathrm{Fmax}}$ are shown in Figures 10 and 11 for the mass-spring systems with Group 1 and 2 resilient materials respectively. In general, $\Delta L_{v,\mathrm{Fmax}}$ and $\Delta L_{p,\mathrm{Fmax}}$ are similar but both curves showing varying degrees of agreement with ΔW_{in}.

For resilient materials B, C and D from Group 1 there is reasonable agreement (up to 3.8 dB

discrepancy) between ΔW_{in}, $\Delta L_{v,\text{Fmax}}$ and $\Delta L_{p,\text{Fmax}}$ between 25 Hz and 125 Hz but not between 200 Hz and 500 Hz. Hence ΔW_{in} is potentially only useful in indicating the change in response in the low-frequency range. However with material A at 80 Hz, ΔW_{in} was significantly larger than $\Delta L_{v,\text{Fmax}}$ and $\Delta L_{p,\text{Fmax}}$. The reason for the lack of agreement between ΔW_{in} with $\Delta L_{v,\text{Fmax}}$ and $\Delta L_{p,\text{Fmax}}$ between 200 Hz and 500 Hz with these relatively soft resilient materials is not known for certain but it might be due to rocking motion of the mass-spring system.

For Group 2, ΔW_{in}, $\Delta L_{v,\text{Fmax}}$ and $\Delta L_{p,\text{Fmax}}$ show close agreement (up to 3.1dB discrepancy) between 25 Hz and 100 Hz and between 250 Hz and 400 Hz but less agreement between 125 Hz and 200 Hz. Hence for these stiffer resilient materials where the mass-spring resonance frequency is above the fundamental mode of the plate, ΔW_{in} is potentially useful in indicating the change in response.

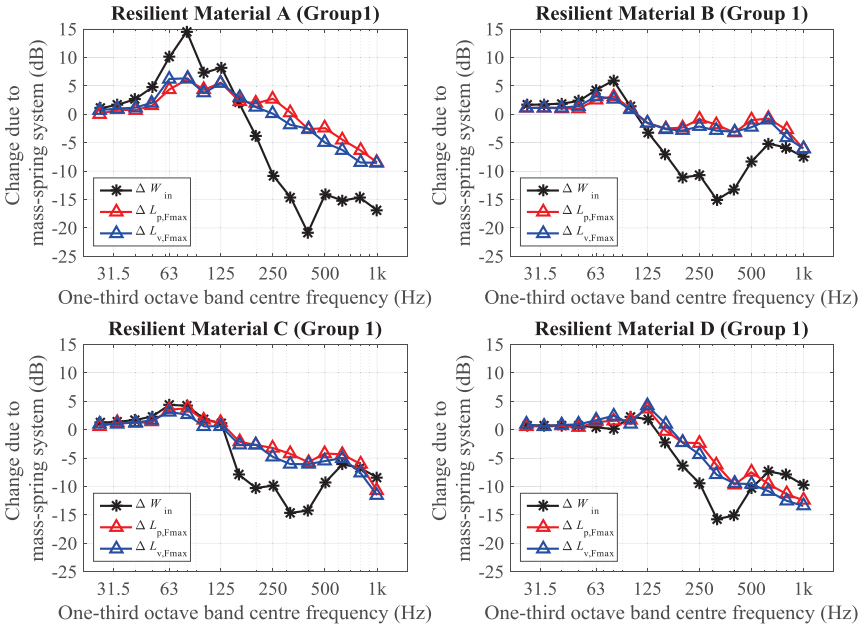

Figure 10. Comparison between differences for transient power input, $L_{v,\text{Fmax}}$ and $L_{p,\text{Fmax}}$ (with minus without a mass-spring system using Group 1 resilient materials).

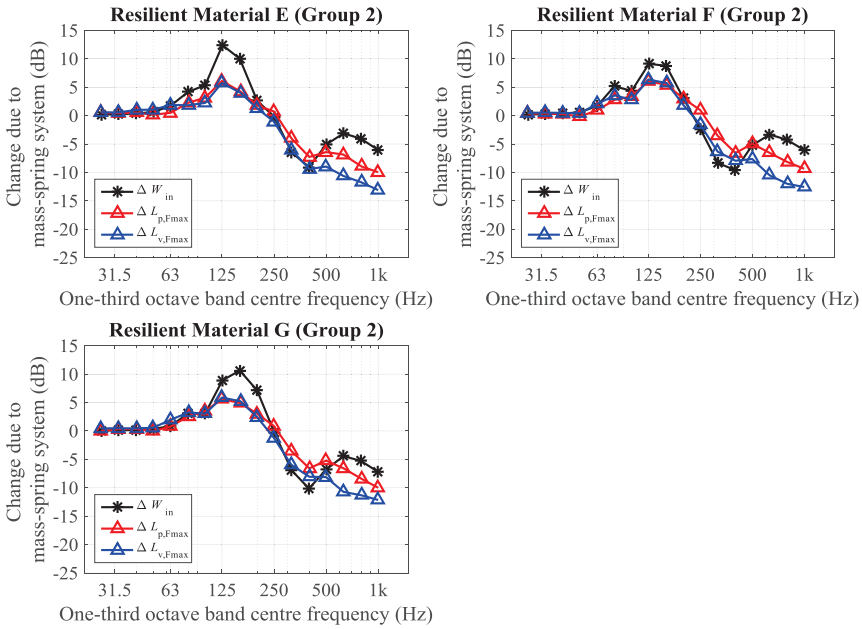

Figure 11. Comparison between differences for transient power input, $L_{v,\text{Fmax}}$ and $L_{p,\text{Fmax}}$ (with minus without a mass-spring system using Group 2 resilient materials).

4. CONCLUSION

For impact sound measurements using a rubber ball, an idealized version of a floating floor is considered using locally-reacting mass-spring systems. Force plate measurements show that the force versus time curve has a single or double hump when the resilient material is dynamically soft or stiff respectively. These features occur with a mass-spring model for the rubber ball and the mass-spring system implemented in Matlab Simulink, but only with optimized material properties. With excitation from the rubber ball with and without a mass-spring system, $L_{v,\mathrm{Fmax}}$ measurements on a concrete base floor and $L_{p,\mathrm{Fmax}}$ measurements in a receiving room indicate that the change in transient power measured using the force plate and the change in $L_{v,\mathrm{Fmax}}$ or $L_{p,\mathrm{Fmax}}$ are only similar when the resilient material is dynamically stiff. For real buildings where resilient materials with a low dynamic stiffness are required it will be necessary to develop a full-scale test to quantify the transient power injected into a base floor to allow implementation of TSEA.

ACKNOWLEDGEMENTS

This research was supported by a grant (16RERP-B082204-03) from Residential Environment Research Program funded by Ministry of Land, Infrastructure and Transport of Korean government.

5. REFERENCES

1. Lee PJ, Kim JH, Jeon JY. Psychoacoustical characteristics of impact ball sounds on concrete floors. Acta Acust united Ac. 2009;95(4):707–17.
2. EN ISO 10140-3:2010+A1:2015 Acoustics – Laboratory measurement of sound insulation of building elements – Part 3: Measurement of impact sound insulation. *International Organization for Standardization.*
3. EN ISO 10140-5:2010+A1:2014 Acoustics – Laboratory measurement of sound insulation of building elements – Part 5: Requirements for test facilities and equipment. *International Organization for Standardization.*
4. JIS A 1418-2: 2000 "Acoustics – Measurement of floor impact sound insulation of buildings – Part 2: Method using standard heavy impact source", Japanese Industrial Standards Committee, 2000.
5. KS F 2810-2:2001 "Method for field measurement of floor impact sound insulation. Part 2: Method using standard heavy impact sources. Korean Standard Committee, South Korea, 2001.
6. Robinson M, Hopkins C. Prediction of maximum time-weighted sound and vibration levels using transient statistical energy analysis. Part 1: Theory and Numerical Implementation. Acta Acust united Ac. 2014;100(1):46–56.
7. Robinson M, Hopkins C. Prediction of maximum time-weighted sound and vibration levels using transient statistical energy analysis. Part 2: Experimental Validation. Acta Acust united Ac. 2014;100(1):57–66.
8. Robinson M, Hopkins C. Prediction of maximum fast time-weighted sound pressure levels due to transient excitation from the rubber ball and human footsteps. Build Environ. 2015;94:810–20.
9. Tanaka H. On the characteristics of heavy weight floor impact source. 1989, Summaries of technical papers of annual meeting Architectural Institute of Japan, 1989. (Japanese Only)
10. Nagurka M, Huang S. A mass-spring-damper model of a bouncing ball. Am Control Conf 2004 Proc 2004. 2004;1(3):499–504.
11. Hubbard M, Stronge WJ. Bounce of hollow balls on flat surfaces. Sport Eng (International Sport Eng Assoc. 2001;4(2):49–61.
12. Schoenwald S, Zeitler, B, Nightingale, T.R.T. Prediction of the Blocked Force at Impact of Japanese Rubber Ball Source. Acta Acust united Ac. 2011;97:590-598.
13. Park B, Jeon JY, Park J. Force generation characteristics of standard heavyweight impact sources used in the sound generation of building floors. J Acoust Soc Am. 2010;128(6):3507–12.
14. EN 29052-1:1992, ISO9052-1:1989 Acoustics – Method for the determination of dynamic stiffness – Part 1: Materials used under floating floors in dwellings. *International Organization for Standardization.*
15. Inman D J. Vibration with Control. John Wiley & Sons, Ltd, Chichester, UK; 2006.
16. uk.mathworks.com. (2016).*Using LTI Arrays for Simulating Multi-Mode Dynamics - MATLAB & Simulink Example*. [online] Available at: http://uk.mathworks.com/help/control/examples/using-lti-arrays-for-simulating-multi-mode-dynamics.html?lang=en [Accessed 03 May. 2016].